Hindawi Publishing Corporation
Journal of Nanotechnology
Volume 2011, Article ID 651971, 6 pages
doi:10.1155/2011/651971

Research Article

An Organic Acid-induced Synthesis and Characterization of Selenium Nanoparticles

Charu Dwivedi, Chetan P. Shah, Krishankant Singh, Manmohan Kumar, and Parma Nand Bajaj

Radiation and Photochemistry Division, Bhabha Atomic Research Centre, Trombay, Mumbai 400 085, India

Correspondence should be addressed to Manmohan Kumar, manmoku@barc.gov.in

Received 30 March 2011; Accepted 26 May 2011

Academic Editor: Mallikarjuna Nadagouda

A simple wet chemical method has been developed to synthesize selenium nanoparticles (size 40–100 nm), by the reaction of sodium selenosulphate precursor with different organic acids in aqueous medium, under ambient conditions. Polyvinyl alcohol has been used to stabilize the selenium nanoparticles. The synthesized nanoparticles can be separated from its sol by using a high-speed centrifuge and can be redispersed in aqueous medium with a sonicator. UV-visible optical absorption spectroscopy, X-ray diffraction, energy dispersive X-rays, differential scanning calorimetry, atomic force microscopy, and transmission electron microscopy techniques have been employed to characterize the synthesized selenium nanoparticles.

1. Introduction

The research on the synthesis and characterization of nanomaterials has been stimulated by their technological applications. The first few technological uses of these materials were as catalysts and pigments. Now, much of the hype surrounding these materials revolves around the enhanced electrical, mechanical, and optical properties. In this nanosize regime, the particles possess short-range structures that are essentially the same as that of the bulk, yet they have optical and/or electronic properties which are dramatically different from that of the bulk [1–3]. These represent a relatively new class of materials and have come under intensive investigations because of their quantum size effects, large surface-to-volume ratio, and the large difference in the properties of their surface atoms. An extensive reported literature exists on the synthesis and applications of nanoparticles of both metals, such as silver, gold, and platinum, and semiconductors, such as CdSe, ZnSe, TiO_2. However, research on metalloid, like selenium, is scanty. Selenium is used in rectifiers, solar cells, photographic exposure meters, and xerography [4]. It is also used in the glass industry to eliminate bubbles and remove undesirable tints produced by iron. Linear and nonlinear optical properties of selenium and its reactivity towards Cd, Zn, make this an important field of study. The research on selenium has attracted more and more attention not only because of its technological applications, but also due to its novel role in life sciences. Selenium is also an essential trace element in human body and has great importance in nourishment and medicine [5]. It exists in a number of crystalline structures, the principal ones being trigonal, consisting of helical chains, and the less stable monoclinic form, consisting of Se_8 rings [6]. Monoclinic Se (m-Se) comes in three forms, α, β, and γ, which differ only in the way the rings are packed [6, 7]. Amorphous selenium (a-Se) is composed of a mixture of disordered chains. Various forms of nanoselenium can be produced, using different synthetic methods [5, 8–12]. Reduction method is the most popular method for selenium nanoparticle preparation, which includes chemical reduction [13], γ-radiolytic reduction [14], bacterial reduction [15], and so forth. However, some literature on the formation of nanoselenium via oxidation method, such as reaction of selenourea with hydroxyl radical [16], electrochemical oxidation of selenide [17], and reaction of sodium selenosulphate with acrylonitrile [18], also exists.

Here, we have developed a new simple wet chemical method, employing protic acids, such as acetic acid, oxalic

acid, and gallic acid to synthesize polyvinyl alcohol-stabilized selenium nanoparticles from aqueous sodium selenosulphate as selenium precursor. The method is capable of producing spherical selenium nanoparticles of size 35 to 70 nm, under ambient conditions. The synthesized selenium nanoparticles were characterized by UV-visible optical absorption spectroscopy, X-ray diffraction (XRD), energy dispersive X-rays (EDAX), differential scanning calorimetry (DSC), atomic force microscopy (AFM), and transmission electron microscopy (TEM) techniques.

2. Experimental Details

High-purity polyvinyl alcohol (PVA) of molecular weight 1,25,000 was obtained from S.D. fine chemicals Ltd., Mumbai, India. All the other chemicals used were of GR grade, procured from local market. Selenium powder was purchased from Aldrich. Aqueous solutions were prepared, using water obtained from Millipore-Q water purification system (with conductivity of 0.6 μScm^{-1}, or less).

Sodium selenosulphate (Na_2SeSO_3) solution was prepared by refluxing a mixture of selenium (2 g) and Na_2SO_3 (20 g) in 100 mL water at 70°C, for about 7 hours [19]. This sodium selenosulphate (Na_2SeSO_3) solution (~ 0.25 mol dm^{-3}), containing unreacted Na_2SO_3, was used as a stock for Se precursor. An aqueous PVA stock solution, 1% by weight, was prepared by dissolving 1.0 g of PVA in 100 mL of water, while stirring at 80°C. The above stock solutions were diluted to the required concentrations for different experiments.

PVA-stabilized Se nanoparticles were synthesized by reaction of sodium selenosulphate (concentration 1×10^{-4} to 1.0×10^{-3} mol dm^{-3}) with different organic carboxylic acids (5×10^{-3} to 3×10^{-2} mol dm^{-3}) in aqueous medium, in the presence of PVA as a stabilizer, in the concentration range from 0.01 to 0.1%. The formation of orange-red-coloured selenium nanoparticle sol was observed in less than one minute. However, in the absence of PVA stabilizer, a dark red-coloured precipitate of selenium was formed.

UV-visible optical absorption spectra of the selenium nanoparticle sols were recorded, using a double beam spectrophotometer, model Spectroscan 2600 from Chemito. XRD patterns of the nanoparticles were recorded with a Phillips X-ray diffractometer, model PW 1710, using a Cu K_α source (λ = 0.15406 nm). DSC measurements were carried out, using a Mettler TA 3000 thermal analysis system (model DSC-30). About 5–10 mg of the synthesized selenium nanoparticles and standard selenium powder were weighed into aluminum crucibles separately, and DSC measurements of both were carried out in N_2 atmosphere, at a heating rate of 10°C/min, from 50° to 250°C. Selenium nanoparticles, separated from aqueous sols, using a high-speed centrifuge, at about 15000 rpm, washed with water, and dried at room temperature, were used for XRD and thermal analysis measurements. AFM analysis of the synthesized selenium nanoparticles was carried out, using a Solver P47 model from NT-MDT, Russia. TEM characterization was carried out with a TECNAI 20, FEI electron microscope, using the sample on a copper grid, coated with a thin amorphous carbon film.

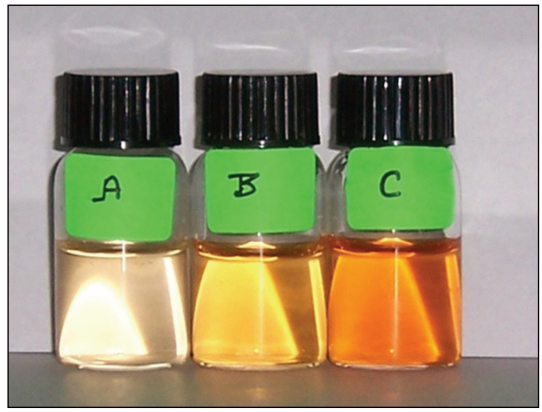

Figure 1: Aqueous selenium nanoparticle sols obtained by the reaction of (A) 2.0×10^{-4} (B) 5.0×10^{-4} (C) 1.0×10^{-3} mol dm^{-3} sodium selenosulphate with 2.0×10^{-2} mol dm^{-3} acetic acid, in the presence of 0.05% PVA.

3. Results and Discussion

3.1. Optical Absorption Studies. The initial concentration of sodium selenosulphate determines the intensity of Se nanoparticle sols. Typical picture of the selenium sols, produced from three different initial concentrations of sodium selenosulphate, is shown in Figure 1.

Figure 2 shows the effect of sodium selenosulphate and PVA concentrations on UV-visible absorption spectra of the selenium nanoparticle sols synthesized by the reaction of sodium selenosulphate with 2.0×10^{-2} mol dm^{-3} of different organic acids. From Figure 2(A), it is clear that the intensity of selenium nanoparticles increases with the increase in sodium selenosulphate concentration. However, it shows a shoulder at around 240 nm, when the reaction was carried out with acetic acid and oxalic acid. But it does not show any such kind of the behavior when the reaction was carried out with an aromatic acid (i.e., gallic acid and many more). This may be due to the overlapping of the absorption spectrum of aromatic system with the shoulder of the selenium nanoparticles, at lower wavelengths (<300 nm). Till now, none of the researchers have observed such a shoulder for selenium nanoparticles. However, the absorbance at lower wavelength region, increases significantly with acid concentration, only in the case of oxalic acid (Figure 2(B)). Whereas, from Figure 2(C), it is clear that, there is no significant effect of PVA concentration, in the concentration range from 0.01 to 0.1%, on the UV-visible absorption spectra of selenium nanoparticles sols. PVA was found to be a very efficient stabilizer for selenium nanoparticles, even at low concentration of 0.01%.

Further, the particle size was correlated with the nature of the UV-visible spectra, and if the particle size is about 100 nm or more, it shows a clear regular maxima in the visible region [20]. Comparison of the present spectra with those reported by Lin and Wang [20] shows that the selenium nanoparticles have an average size of about 80 nm, which is further supported by AFM images.

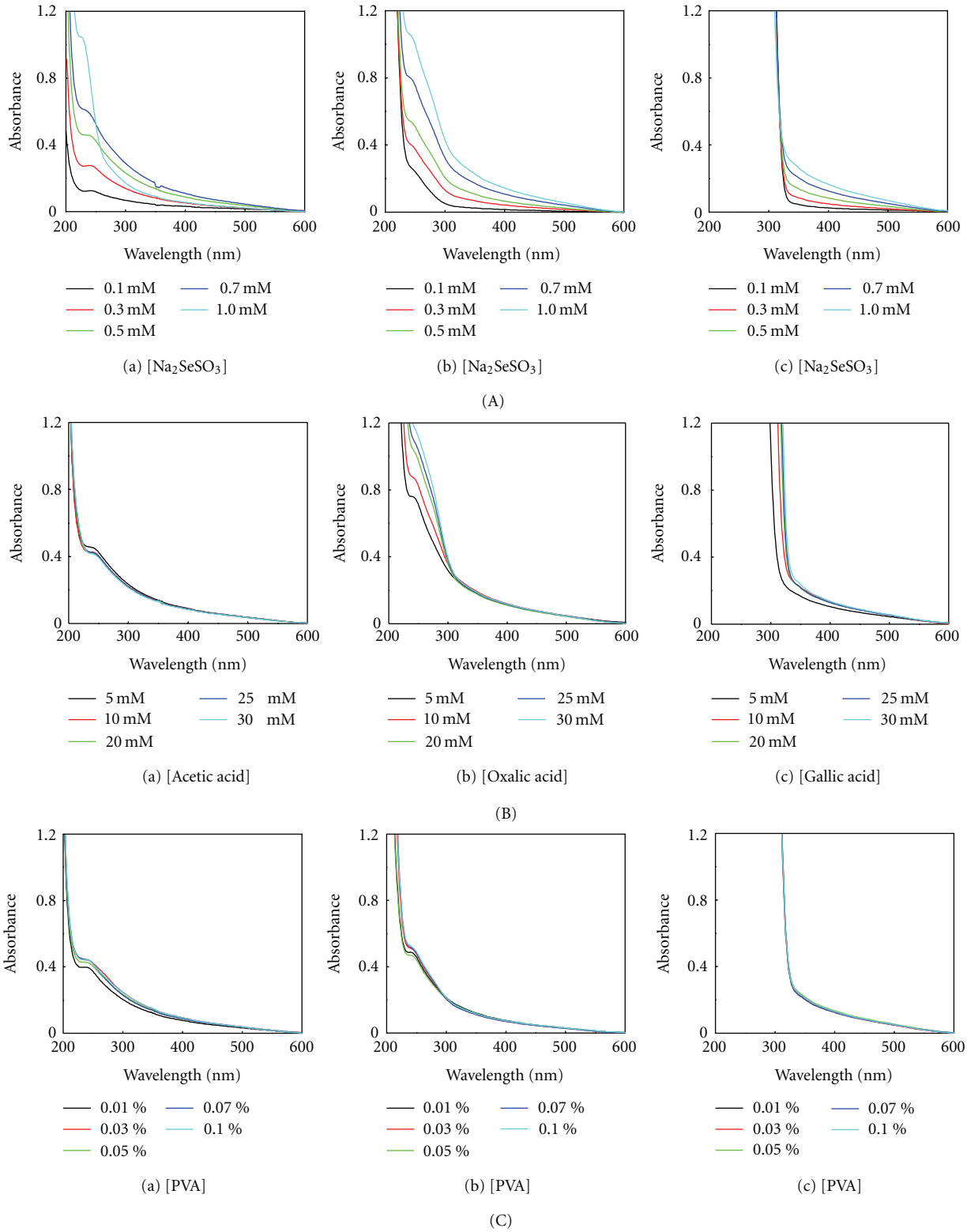

Figure 2: (A) Effect of sodium selenosulphate concentration on the UV-visible absorption spectra of the selenium sols produced by the reaction of sodium selenosulphate with 5.0×10^{-3} mol dm^{-3} (a) acetic acid, (b) oxalic acid, and (c) gallic acid, at a fixed concentration of PVA (0.05%). (B) Effect of acid concentration, (a) acetic acid, (b) oxalic acid, and (c) gallic acid, on the absorption spectra of the selenium sols produced by reaction with 5.0×10^{-4} mol dm^{-3} sodium selenosulphate, in the presence of 0.05% PVA. (C) Effect of PVA concentration on absorption spectra of the selenium sol produced by the reaction of 5.0×10^{-4} mol dm^{-3} sodium selenosulphate with 5.0×10^{-3} mol dm^{-3} (a) acetic acid, (b) oxalic acid, and (c) gallic acid.

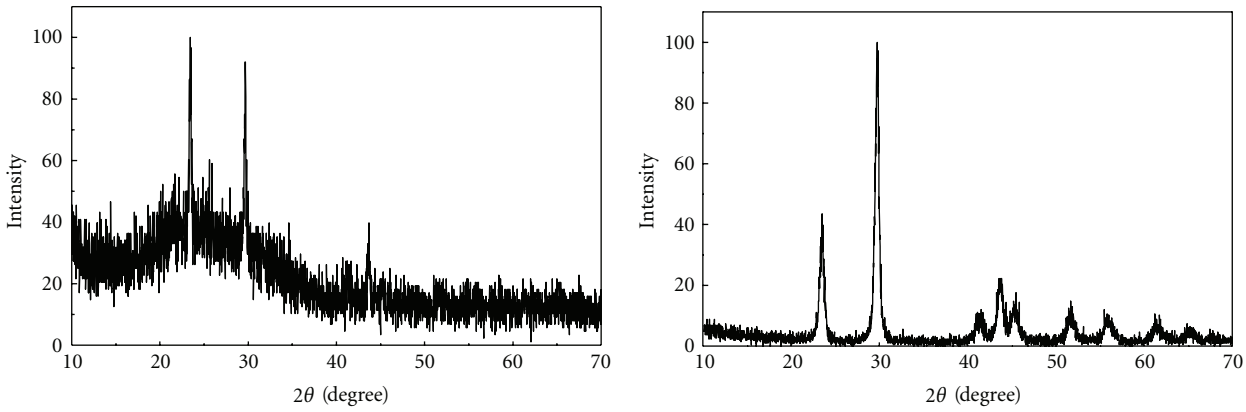

Figure 3: (a) XRD pattern of the synthesized selenium nanoparticles annealed at 130°C, for 6 hrs, and (b) commercial selenium sample. Selenium nanoparticles were synthesized by the reaction of 1.0×10^{-3} mol dm^{-3} sodium selenosulphate with 2.0×10^{-2} mol dm^{-3} acetic acid, in the presence of 0.01% PVA.

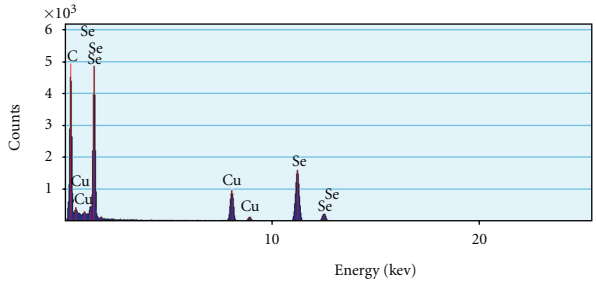

Figure 4: EDAX pattern of the selenium nanoparticles, synthesized by the reaction of 1.0×10^{-3} mol dm^{-3} sodium selenosulphate with 2.0×10^{-2} mol dm^{-3} acetic acid, in the presence of 0.01% PVA.

3.2. X-Ray Diffraction Study and EDAX of the Synthesized Selenium Nanoparticles. Crystal structure of the selenium nanoparticles was determined by XRD technique. The typical XRD patterns of the synthesized sample, after heat treatment at 130°C, for 6 hrs, and that of the commercially available selenium, are displayed in Figures 3(a) and 3(b), respectively. The XRD pattern of the synthesized selenium nanoparticles, without heat treatment, is much more noisy, with broader peaks (plot not shown), indicating amorphous nature of the particles. It is believed that amorphous selenium is red in colour, which is further confirmed by selenium sol presented in Figure 1. All the diffraction pattern peaks in Figure 3(a) correspond to trigonal phase, with lattice constants $a = 4.362$ Å and $c = 4.958$ Å, which match very well with the reported values (JCPDS file no. 06-362).

Further, chemical composition of the synthesized selenium nanoparticles was also confirmed by EDAX. The EDAX spectrum of the nanoparticles, shown in Figure 4, also indicates that the nanoparticles are of selenium only. The peak corresponding to copper and carbon arises due to carbon-coated copper grid, on which thin film of the sample was deposited for TEM analysis.

3.3. Differential Scanning Calorimetry (DSC) Study. DSC thermograms of the synthesized selenium nanoparticles and standard commercial selenium sample were recorded from 50° to 250°C. DSC thermogram of the synthesized selenium nanoparticles showed an exothermic transition at 90°C, along with endothermic melting peak at 217°C (Figure 5(a)). Enthalpy of the transition was found to be 45.2 J/g. The repeat DSC thermogram of the same selenium sample, recorded after bringing it to ambient temperature, did not show any exothermic peak at the mentioned temperature (plot not shown). This clearly indicates that the selenium particles loose their nanocrystalline nature in the first thermal run itself, and the transition could be assigned to increase in the crystallinity of the selenium nanoparticles. This observation is in corroboration with the XRD results obtained with the synthesized sample and that annealed at 130°C. DSC thermogram of the standard selenium powder sample also shows melting peak at 217°C, without any such exothermic peak, which is shown in Figure 5(b).

3.4. AFM and TEM Studies. AFM and TEM are very important techniques, which are used to get the information about particle size, shape, surface topography, and so forth. Therefore, morphology and structure of the synthesized selenium nanoparticles were also determined by these techniques. Typical 2D and 3D AFM images of the synthesized selenium nanoparticles are shown in Figure 6. The 2D image of the synthesized selenium nanoparticles shows smaller individual particles of about 10 nm size, along with larger agglomerates of sizes upto ~150 nm while the 3D image indicates the presence of individual spherical particles, with maximum height of 30 nm in the z-direction.

Transmission electron microscope image of the synthesized selenium nanoparticle is shown in Figure 7. Spherical shape of individual nanoparticles, with size in the range of 35–70 nm, is evident from the TEM image. AFM image is taken by suspending much higher concentration of the

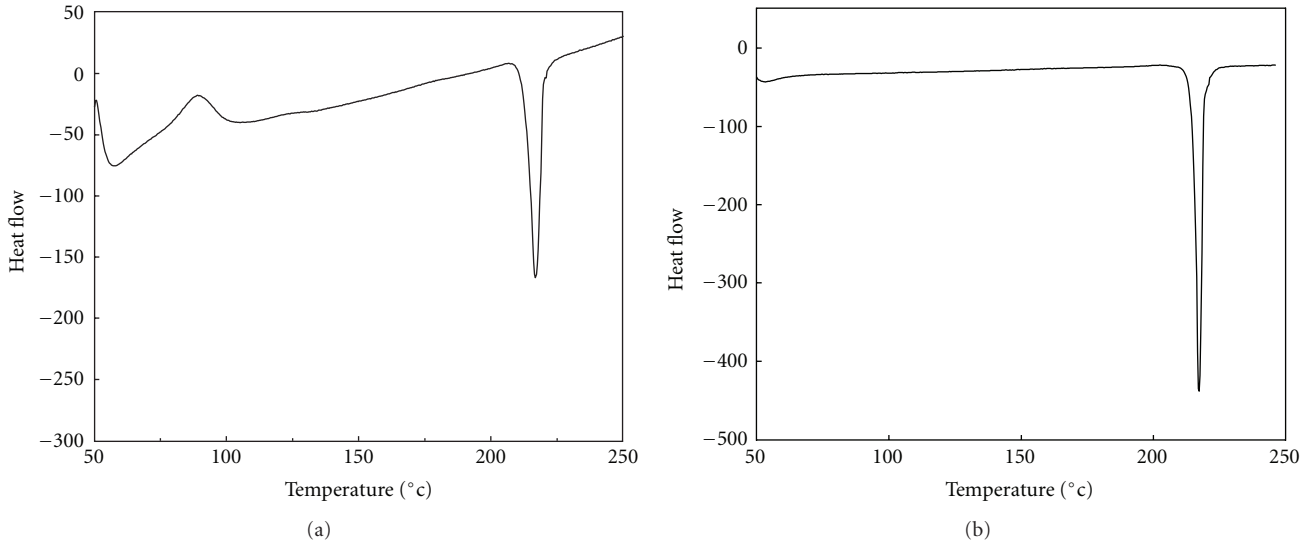

Figure 5: DSC thermogram of (a) the selenium nanoparticles synthesized by the reaction of 1.0×10^{-3} mol dm^{-3} sodium selenosulphate with 2.0×10^{-2} mol dm^{-3} acetic acid, in the presence of 0.01% PVA, and (b) standard commercial selenium sample.

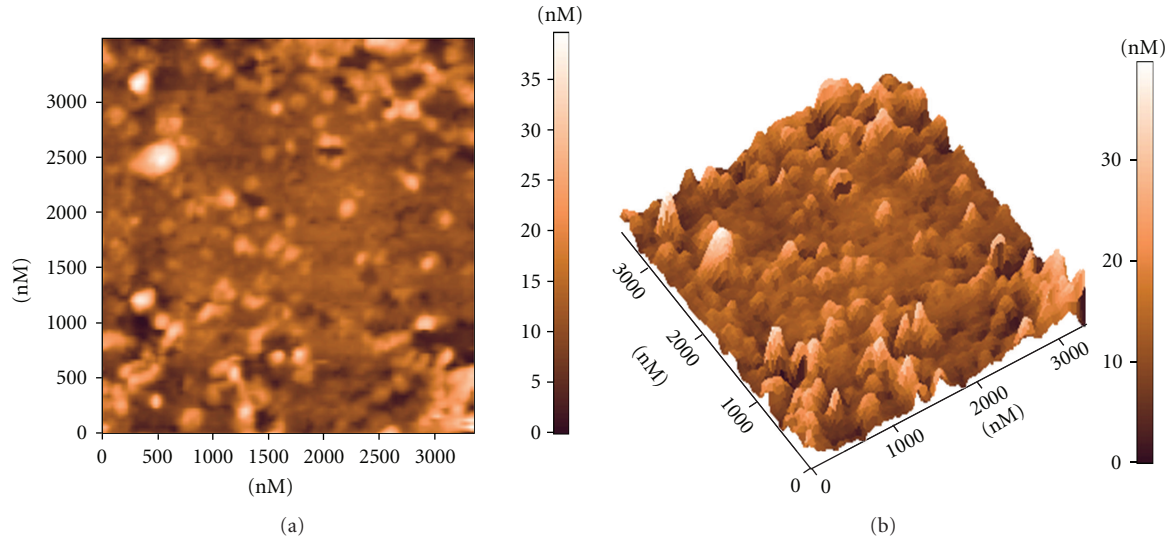

Figure 6: AFM images of the selenium nanoparticles formed by the reaction of 1.0×10^{-3} mol dm^{-3} sodium selenosulphate with 2.0×10^{-2} mol dm^{-3} acetic acid, in the presence of 0.01 % PVA, (a) 2D image and (b) 3D image.

selenium nanoparticles on the silicon wafer in the presence of the PVA stabilizer. It shows individual particles in the size range of 10–150 nm, along with some larger aggregates while the TEM image is taken at much higher magnification, with a dilute sample, after washing out the PVA stabilizer. Thus, it shows a specific portion of the sample deposited on the graphite-coated copper grid, having well-separated individual particles of size in the range of 35–70 nm. These differences in the two sample preparation methods are responsible for the observed difference in the particle sizes. The conclusions drawn from AFM and TEM studies are in corroboration with each other. Thus, the present method is capable of producing spherical selenium nanoparticles.

4. Conclusions

Acid-induced synthesis of selenium nanoparticles has been found to be a simple and convenient method, which can be carried out under ambient conditions. PVA was used as a stabilizer for the selenium nanoparticles. The size of the selenium particles was found to increase with sodium selenosulphate concentration. The effects of higher concentration of PVA and organic acids were not that pronounced. Nanonature of the synthesized selenium particles and increase in their crystallinity on heating were confirmed by both XRD and DSC experiments. Spherical selenium nanoparticles of size about 35–70 nm, as determined by AFM and TEM techniques, could be produced. The

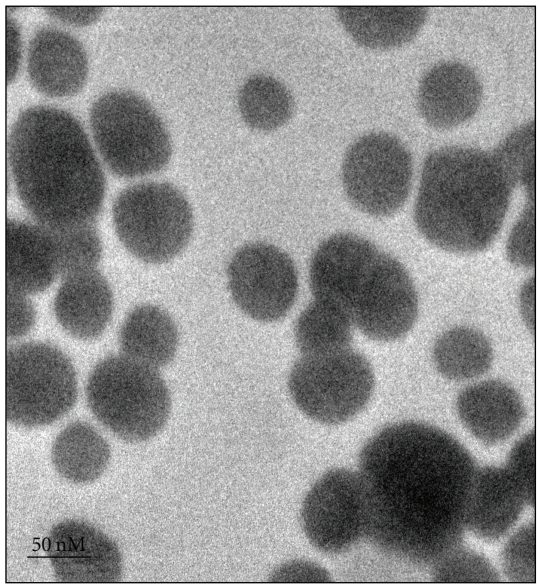

Figure 7: TEM images of the selenium nanoparticles, formed by the reaction of 1.0×10^{-3} mol dm^{-3} sodium selenosulphate with 2.0×10^{-2} mol dm^{-3} acetic acid, in the presence of 0.01% PVA.

selenium nanoparticles may serve as template, to generate other important nanomaterials, and find applications in fabrication of nanoscale optoelectronic devices.

Acknowledgments

The author, C. Dwivedi, is grateful to Homi Bhabha National Institute, BRNS, and Department of Atomic Energy, for awarding research fellowship. The authors are thankful to Dr. P. A. Hassan, BARC, for AFM, Dr. S. C. Purandare and Mr. R. D. Bapat, TIFR, for TEM and EDAX, and Dr. L. Varshney, BARC, for DSC experiments. The authors also wish to acknowledge Dr. T. Mukherjee and Dr. S. K. Sarkar, for their encouragement during the course of the study.

References

[1] Y. Wang and N. Herron, "Nanometer-sized semiconductor clusters: materials synthesis, quantum size effects, and photophysical properties," *Journal of Physical Chemistry*, vol. 95, no. 2, pp. 525–532, 1991.

[2] M. Haase, H. Weller, and A. Henglein, "Photochemistry of colloidal semiconductors. 26. Photoelectron emission from CdS particles and related chemical effects," *Journal of Physical Chemistry*, vol. 92, no. 16, pp. 4706–4712, 1988.

[3] R. Rossetti and L. E. Brus, "Picosecond resonance Raman scattering study of methylviologen reduction on the surface of photoexcited colloidal CdS crystallites," *Journal of Physical Chemistry*, vol. 90, no. 4, pp. 558–560, 1986.

[4] S. Li, Y. Shen, A. Xie et al., "Rapid, room-temperature synthesis of amorphous selenium/protein composites using Capsicum annuum L extract," *Nanotechnology*, vol. 18, no. 40, Article ID 405101, 2007.

[5] X. Cao, Y. Xie, S. Zhang, and F. Li, "Ultra-thin trigonal selenium nanoribbons developed from series-wound beads," *Advanced Materials*, vol. 16, no. 7, pp. 649–578, 2004.

[6] P. Cherin and P. Unger, "The crystal structure of trigonal selenium," *Inorganic Chemistry*, vol. 6, no. 8, pp. 1589–1591, 1967.

[7] P. Ungar and P. Cherin, in *The Physics of Selenium and Tellurium*, W. C. Cooper, Ed., p. 223, Pergamon, Oxford, UK, 1969.

[8] P. Cherin and P. Ungar, "Refinement of crystal structure of α-monoclinic Se," *Acta Crystallographica*, vol. 28, pp. 313–317, 1972.

[9] H. Yin, Z. Xu, H. Bao, J. Bai, and Y. Zheng, "Single crystal trigonal selenium nanoplates converted from selenium nanoparticles," *Chemistry Letters*, vol. 34, no. 1, pp. 122–123, 2005.

[10] J. Xu, F. Yang, L. Chen, Y. Hu, and Q. Hu, "Effect of selenium on increasing the antioxidant activity of tea leaves harvested during the early spring tea producing season," *Journal of Agricultural and Food Chemistry*, vol. 51, no. 4, pp. 1081–1084, 2003.

[11] B. Zhang, X. Ye, W. Dai, W. Hou, F. Zuo, and Y. Xie, "Biomolecule-assisted synthesis of single-crystalline selenium nanowires and nanoribbons via a novel flake-cracking mechanism," *Nanotechnology*, vol. 17, no. 2, pp. 385–390, 2006.

[12] P. Liu, Y. Ma, W. Cai et al., "Photoconductivity of single-crystalline selenium nanotubes," *Nanotechnology*, vol. 18, no. 20, Article ID 205704, 2007.

[13] Q. Li and V. W. W. Yam, "High-yield synthesis of selenium nanowires in water at room temperature," *Chemical Communications*, no. 9, pp. 1006–1008, 2006.

[14] Y. Zhu, Y. Qian, H. Huang, and M. Zhang, "Preparation of nanometer-size selenium powders of uniform particle size by γ-irradiation," *Materials Letters*, vol. 28, no. 1–3, pp. 119–122, 1996.

[15] R. S. Oremland, M. J. Herbel, J. S. Blum et al., "Structural and Spectral Features of Selenium Nanospheres Produced by Se-Respiring Bacteria," *Applied and Environmental Microbiology*, vol. 70, no. 1, pp. 52–60, 2004.

[16] B. Mishra, P. A. Hassan, K. I. Priyadarsini, and H. Mohan, "Reactions of biological oxidants with selenourea: formation of redox active nanoselenium," *Journal of Physical Chemistry B*, vol. 109, no. 26, pp. 12718–12723, 2005.

[17] T. C. Franklin, W. K. Adeniyi, and R. Nnodimele, "Electro-oxidation of some insoluble inorganic sulfides, selenides, and tellurides in cationic surfactant-aqueous sodium hydroxide systems," *Journal of the Electrochemical Society*, vol. 137, no. 2, pp. 480–484, 1990.

[18] C. P. Shah, M. Kumar, K. K. Pushpa, and P. N. Bajaj, "Acrylonitrile-induced synthesis of polyvinyl alcohol-stabilized selenium nanoparticles," *Crystal Growth and Design*, vol. 8, no. 11, pp. 4159–4164, 2008.

[19] S. Gorer and G. Hodes, "Quantum size effects in the study of chemical solution deposition mechanisms of semiconductor films," *Journal of Physical Chemistry*, vol. 98, no. 20, pp. 5338–5346, 1994.

[20] Z. H. Lin and C. R. C. Wang, "Evidence on the size-dependent absorption spectral evolution of selenium nanoparticles," *Materials Chemistry and Physics*, vol. 92, no. 2-3, pp. 591–594, 2005.